

Light-induced magnetic trapping for cold alkali atoms using a combined optical tweezers and nanofibre platform

Alexey Vylegzhanin,* Dylan J. Brown, Sergey Abdrakhmanov, and Sile Nic Chormaic†
Light-Matter Interactions for Quantum Technologies Unit,

Okinawa Institute of Science and Technology Graduate University, Onna, Okinawa 904-0495, Japan.

(Dated: December 11, 2024)

We present a magnetic trapping method for cold ^{87}Rb atoms, utilising the light-induced magnetic fields from the evanescent field of an optical nanofibre (ONF) in conjunction with an optical tweezers. We calculate and plot the trapping potentials for both Gaussian and Laguerre-Gaussian modes of the optical tweezers, and quasi-linear polarisation of the ONF-guided field. Based on the optical powers in the tweezers beam and the ONF-guided mode, we analyse the trap depths and the distances of the trap minima from the surface of the nanofibre. We show that, by controlling the powers in both of the optical fields, one can vary the trap position over a few hundreds of nanometres, while also influencing the trap depth and trap frequencies. Such control over atom position is essential both for studying distance-dependent effects on atoms trapped near dielectric surfaces, and minimising these effects for quantum technology applications.

I. INTRODUCTION

In recent years, there has been growing interest in trapping and optically interfacing cold, neutral atoms near optical waveguides [1–8]. One highly efficient trapping method uses optical dipole forces from blue- and red-detuned evanescent light fields of an optical nanofibre (ONF), forming what is referred to as a two-colour trap [1]. There have been several experimental realisations of such a scheme for laser-cooled Cs [2, 9, 10] and Rb [11, 12] atoms. Aside from trapping, the evanescent field can be used to probe atoms near the fibre [13–18] or for the excitation of atoms to Rydberg states [19–23]. The latter technique is promising for quantum computation or the realisation of quantum networks/repeaters [8, 24–28].

Another rapidly developing platform for trapping and manipulating cold atoms in well-controlled sites is that of free-space optical tweezers [29–33]. Such systems have been extended to the trapping of Rydberg atoms [34, 35]. The advantage of optical tweezers lies in their ability to trap a large number of atoms simultaneously in complex 1D, 2D, or 3D arrays, and their integration into cold atom setups is very well-established. In addition, optical tweezers can be combined with optical waveguides, such as optical nanofibres [36] or photonic crystal waveguides [37], to trap atoms near the waveguide surface, providing enhanced coupling into the guided mode. However, such a scheme relies on the reflection of the optical tweezers beam from the waveguide itself, leading to the atom being trapped at a fixed distance from the surface. The position of the trap minimum can be changed by varying the geometric parameters of the waveguide (which is impossible to do in situ), by tuning the tweezers wavelength over hundreds of nanometers (only possible if us-

ing widely tunable lasers) or by changing the beam polarisation [37], for which the fastest achievable time is on the order of μs [38].

In this work, we propose a method to trap ground state, laser-cooled ^{87}Rb atoms in a light-induced magnetic field trap, formed by combining the evanescent field of an ONF with a circularly polarised optical tweezers beam consisting of either a Gaussian or a Laguerre-Gaussian (LG) mode. Atoms in an electromagnetic field with nonzero ellipticity experience a light-induced fictitious magnetic field [39–41]. In our proposed trapping scheme, both the evanescent field and the optical tweezers have nonzero ellipticity and, therefore, produce a light-induced magnetic field for the atoms. We set the polarisation of the ONF-guided light and the optical tweezers so that a local minimum of the magnetic field is formed. The distance between the ONF surface and the position of the trap minimum can be adjusted by changing the power of either the ONF-guided field or the optical tweezers field using acousto-optical modulators (AOMs) on timescales of μs comparable to current optical tweezers experiments for cold, neutral atoms [32, 42].

II. LIGHT-INDUCED MAGNETIC FIELD

An atom in an oscillating electromagnetic field experiences an AC-Stark shift, which depends on the strength of the electric field and the atom's frequency-dependent polarisability, thereby shifting the energy levels. This polarisability can be represented by the scalar, vector, and tensor components of the polarisability tensor [43]. By using a tune-out wavelength, the scalar light shift can be minimised to near zero, leaving only the vector and tensor light shifts. For the ^{87}Rb ground state, $5S_{1/2}$, the tensor light shift is zero, and the tune-out wavelength is approximately 790.2 nm [44]. At this wavelength, the scalar light shifts from the D_1 and D_2 transitions cancel each other out in the $5S_{1/2}$ state, resulting in a net zero shift. Consequently, the only remaining component is the

* alexey.vylegzhanin@oist.jp

† sile.nicchormaic@oist.jp

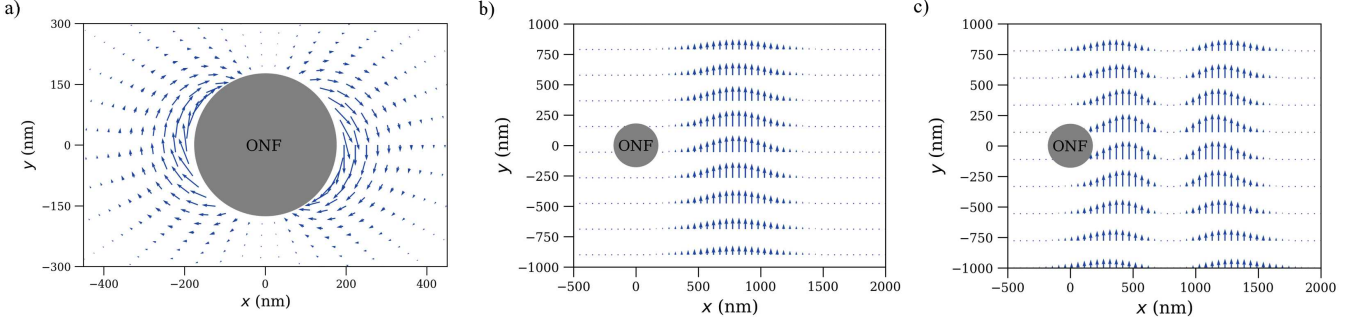


FIG. 1. Vector field of the light-induced magnetic field (blue arrows) for an atom in the $|5P_{1/2}, F = 2, m_F = 2\rangle$ state in the xy plane perpendicular to the fibre for: (a) a quasi-linearly polarised fundamental ONF guided mode, (b) a circularly polarised Gaussian mode, and (c) an LG_{01} mode tweezers. The fibre radius is $a = 175$ nm and the free-space wavelength of the ONF guided mode is $\lambda_{\text{ONF}} = 787.3$ nm. The waist, w_0 , is 500 nm, the distance between the centre of the beam and the ONF surface is 625 nm, the power of the beam is 0.3 mW and the free-space wavelength is $\lambda_{\text{tw}} = 790.2$ nm. One can see that the LG mode tweezers beam produces a larger light-induced magnetic field closer to the fibre surface.

vector light shift, which can be written as

$$\Delta E_{\text{AC}}^{\text{v}} = \frac{1}{4} \alpha_{nJF}^{\text{v}} i [\mathcal{E}^* \times \mathcal{E}] \frac{m_F}{2F}. \quad (1)$$

The vector light shift depends on the magnetic quantum number, m_F , and can be interpreted as the magnetic potential $U_{\text{mag}} = \mu_{\text{B}} g_{nJF} m_F |\mathbf{B}_{\text{fict}}|$, where \mathbf{B}_{fict} is a light-induced or fictitious magnetic field, expressed by [41, 43]

$$\mathbf{B}_{\text{fict}} = \frac{\alpha_{nJF}^{\text{v}}}{8\mu_{\text{B}} g_{nJF} F} i [\mathcal{E}^* \times \mathcal{E}]. \quad (2)$$

Here, μ_{B} is the Bohr magneton, n is the principle quantum number, J is the total angular momentum quantum number, F is the hyperfine splitting quantum number, g_{nJF} is the Landé g-factor, m_F is the Zeeman splitting atomic level, α_{nJF}^{v} is the frequency-dependent vector polarisability of an atom in the $|nJF\rangle$ state, and \mathcal{E} is the positive-frequency electric field envelope of the complex electric field, $\mathbf{E} = 1/2 (\mathcal{E} e^{-i\omega t} + \text{c.c.})$.

III. LIGHT-INDUCED MAGNETIC TRAP

To model the trap we introduce an optical nanofibre made of silica with refractive index $n = 1.44$ and radius $a = 175$ nm. A fibre of this radius only supports the HE_{11} mode of the 790.2 nm light used in this work [45, 46]. A significant portion of the guided light extends outside the optical nanofibre in the form of an evanescent field [47]. We set the polarisation of the guided mode to quasi-linear along the z -axis in the ONF region, meaning that there are only z and x components of the electric field.

The light-induced magnetic field presented in equation 2, created by an ONF guided mode, can be expressed

in cylindrical coordinates as

$$\mathbf{B}_{\text{fict}} = \frac{\alpha_{nJF}^{\text{v}}}{4\mu_{\text{B}} g_{nJF} F} [\text{Im}(\mathcal{E}_z \mathcal{E}_r^*) \hat{\phi} + \text{Im}(\mathcal{E}_r \mathcal{E}_\phi^*) \hat{z} + \text{Im}(\mathcal{E}_\phi \mathcal{E}_z^*) \hat{r}], \quad (3)$$

where $\mathcal{E}_{\text{circ}}^{(fp)} = (\mathcal{E}_r, \mathcal{E}_\phi, \mathcal{E}_z)$ represents the radial, azimuthal, and longitudinal cylindrical components of the electric field of the nanofibre guided mode that are precisely described by Le Kien *et al.* [46]. In the case of the quasi-linearly (QL) polarised guided mode of the ONF, the fictitious magnetic field can be simplified to the following form

$$\mathbf{B}_{\text{fict}J} = \frac{\alpha_{nJ}^{\text{v}}}{4\mu_{\text{B}} g_{nJ} J} [\text{Im}(\mathcal{E}_{z,\text{lin}} \mathcal{E}_{r,\text{lin}}^*) \hat{\phi} + \text{Im}(\mathcal{E}_{\phi,\text{lin}} \mathcal{E}_{z,\text{lin}}^*) \hat{r}], \quad (4)$$

where \mathcal{E}_{lin} is the electric field of a linearly polarised mode and is written as a summation of opposite handedness quasi-circular (QC) polarisation guided modes

$$\mathcal{E}_{\text{lin}}^{(f\phi_{\text{pol}})} = \frac{1}{\sqrt{2}} (\mathcal{E}_{\text{circ}}^{(f+)} e^{-i\phi_{\text{pol}}} + \mathcal{E}_{\text{circ}}^{(f-)} e^{i\phi_{\text{pol}}}). \quad (5)$$

Here, $\mathcal{E}_{\text{circ}}$ is the electric field of the QL guided mode, ϕ_{pol} is the polarisation angle with respect to the x -axis, f is either $+1$ or -1 and determines the propagation direction, with $+$ and $-$ defining the handedness of the QC guided mode [48]. A vector plot of the light-induced magnetic field from the QL guided mode of the ONF is shown in Fig. 1(a).

The polarisation of the optical tweezers beam is set to anti-clockwise in the xz plane while the Poynting S -vector is set along the y direction. Therefore the light-induced magnetic field is directed along the y -axis. We set the centre of the optical tweezers at 625 nm from the surface of the ONF and the waist of the tweezers beam, w_0 , to 500 nm. The power of the optical tweezers is set to

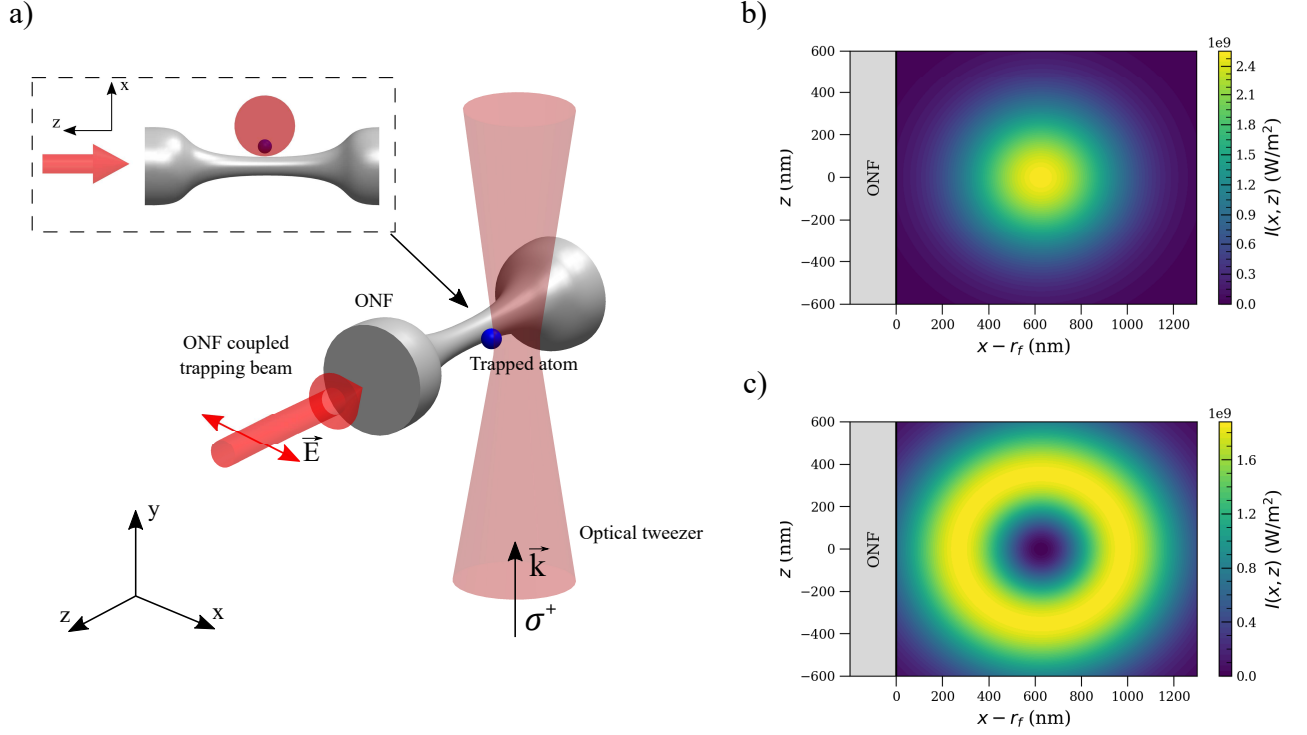


FIG. 2. (a) Schematic image of the setup. One light beam (intense red arrow) at the free-space wavelength, $\lambda_{\text{ONF}} = 787.3$ nm, is coupled into the nanofibre. Only the fundamental, quasi-linearly polarised guided mode (\vec{E}) propagates through the ONF region. An optical tweezers (faint red) Gaussian or Laguerre-Gaussian doughnut mode beam is focussed at $d = 625$ nm distance from the fibre surface. The waist, w_0 , of the focussed beam is 500 nm. The free-space wavelength is $\lambda_{\text{ONF}} = 790.2$ nm. The atom (blue sphere) is trapped between the ONF surface and the centre of the tweezers beam due to the interaction with both the focussed tweezers light and the evanescent field of the ONF guided mode. \vec{k} is the propagation direction and σ^+ is the polarisation of the tweezers beam. Inset - view in the xz plane at $y = 0$. (b,c) Two-dimensional intensity profiles, $I(x, z)$, of the Gaussian mode and the Laguerre-Gaussian mode with 1 mW of power in (x, z) plane at $y = 0$ respectively.

0.3 mW. The schematic of the setup with the ONF and the optical tweezers arrangement is shown in Fig. 2(a).

The intensity of the optical tweezers shown on the Fig. 2(b) can be written in the form [49]

$$I(x, y, z) = I_0 \left(\frac{w_0}{w(y - y_c)} \right)^2 e^{\frac{-2\rho^2}{w^2(y - y_c)}}, \quad (6)$$

$$\rho = \sqrt{(x - x_c)^2 + (z - z_c)^2}$$

where

$$w(y) = w_0 \sqrt{1 + \left(\frac{y - y_c}{y_R} \right)^2}, \quad (7)$$

$$y_R = \frac{\pi w_0^2}{\lambda},$$

$$I_0 = \frac{2P_0}{\pi w_0^2}.$$

Here, w_0 is the radius of the tweezers beam at the waist, $w(y)$ is the radius of the beam along the y -axis, I_0 is the intensity of the beam at the centre, y_R is the Rayleigh length, P_0 is the power of the beam, (x_c, y_c, z_c) are coordinates of the beam centre. Since

$|E(x, y, z)|^2 = 2\eta_0 I(x, y, z)$ and based on the equation 2, the light-induced magnetic field therefore can be written in the following form [41, 50, 51]

$$\mathbf{B}_{\text{fict}}^{\text{tw}} = 2\eta_0 I \frac{\alpha_{nJF}^y}{8\mu_B g_{nJ}} \hat{e}_y, \quad (8)$$

where the vacuum wave impedance $\eta_0 = 377$ Ohm.

The magnetic field direction for the optical tweezers is along the direction of beam propagation, i.e. the y -axis. The vector plot of the light-induced magnetic field from the Gaussian mode tweezers beam in the xy plane is shown in Fig. 1(b). Optical tweezers atom traps with a circularly polarised electric field were analysed in [50]

For optical tweezers, one can also use a Laguerre-Gaussian (LG) mode or a Hermite-Gaussian (HG) mode to modify the electric field profile allowing the high-intensity region to be brought closer to the fibre surface. The intensity of a doughnut mode LG_{01} ($p = 1, l = 0$)

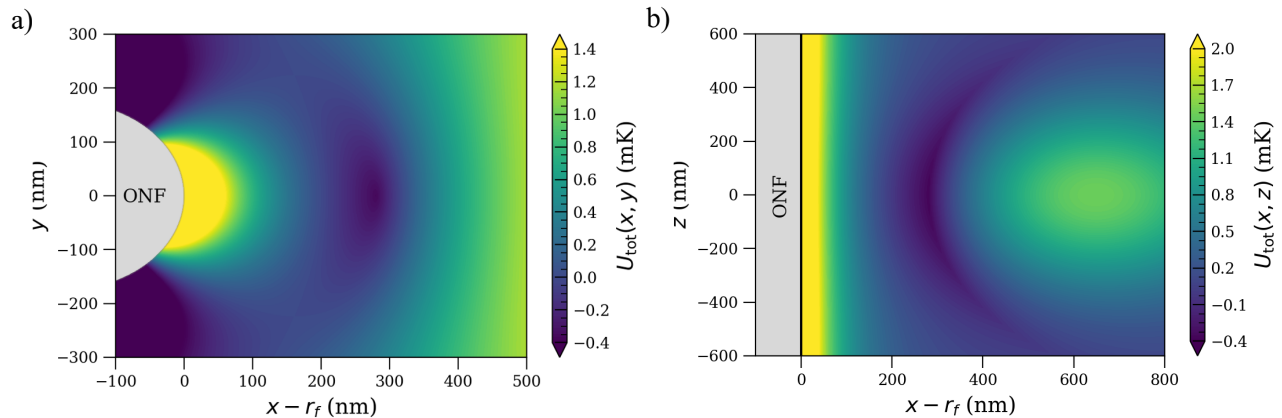


FIG. 3. Two-dimensional plots of the light-induced magnetic field trapping potential (a) $U_{\text{tot}}(x, y)$ and (b) $U_{\text{tot}}(x, z)$ for a ^{87}Rb atom in the $|5S_{1/2}, F = 2, m_F = 2\rangle$ ground state. The potential is formed by a quasi-linearly polarised fibre guided mode with $P_{\text{ONF}} = 1$ mW and a Gaussian mode tweezers beam with $P_{\text{tw}} = 0.3$ mW. The potential minimum is formed at ~ 280 nm from the fibre surface and the trap depth is ~ 0.37 mK. The free-space wavelengths are $\lambda_{\text{ONF}} = 787.3$ nm and $\lambda_{\text{tw}} = 790.2$ nm for the fibre guided mode and tweezers mode, respectively. The fibre radius is $r_f = 175$ nm. Each plot has an offset so that the lowest point represents the trap depth. The trap depth is defined as the minimum potential barrier of the three-dimensional potential $U_{\text{tot}}(x, y, z)$.

shown on the Fig. 2(c) beam can be written as [49]

$$I_{\text{LG}} = I_0^{\text{LG}} \cdot \psi_{\text{LG}},$$

$$\psi_{\text{LG}}(x, y, z) = \left(\frac{w_0}{w(y - y_c)} \right)^2 \left(\frac{2\rho^2}{w^2(y - y_c)} \right) e^{\frac{-2\rho^2}{w^2(y - y_c)}},$$

$$\rho = \sqrt{(x - x_c)^2 + (z - z_c)^2} \quad (9)$$

where $w(y)$ and y_R can be taken from equation 7 and (x_c, y_c, z_c) are coordinates of the beam centre. The peak intensity for the Laguerre-Gaussian mode, I_0^{LG} , is calculated from the beam power normalisation equation

$$I_0^{\text{LG}} = \frac{P_0}{\iint \psi_{\text{LG}}(x, z) dx dz}, \text{ at } y = 0 \quad (10)$$

The light-induced magnetic field from the LG_{01} beam can be expressed via equation 8. To introduce a circular polarisation in the xz plane for the LG_{01} beam one has to overlap two LG_{01} beams with radial and azimuthal polarisations. In this case, the light-induced field will be oriented along the y -axis as stated in equation 8. The vector plot of the light-induced magnetic field from the LG_{01} mode tweezers beam in the xy plane is shown in Fig. 1(c).

When an atom is introduced into a combination of different fictitious magnetic fields, or a combination of a fictitious and a real magnetic field, the total magnetic field can be calculated as a vector sum [51, 52] with the resultant field defining the quantisation axis, such that $\mathbf{B}_{\text{eff}} = \mathbf{B}_{\text{fict}} + \mathbf{B}_{\text{fict}}^{\text{tw}}$, which has been demonstrated in experiments [52, 53]. From Fig. 1, it can be seen that the fictitious magnetic fields produced by the ONF and the optical tweezers have opposite directions on the positive x side of the fibre and therefore the total magnetic

field, \mathbf{B}_{eff} , has a minimum amplitude at some distance from the ONF surface. Hence, the magnetic potential an atom experiences is

$$U_{\text{mag}} = -\boldsymbol{\mu} \cdot \mathbf{B}_{\text{eff}}, \quad (11)$$

where $\boldsymbol{\mu}$ is the magnetic moment of the atom [40]. Here, the potential is formed for low-field seeking atoms. We set the quantisation axis along the y -axis by a bias magnetic field of 5 G. Hence, the magnetic moment of the atom remains anti-parallel to the local effective magnetic field during atomic motion in the trap and the trapping potential can be simplified to

$$U_{\text{mag}} = \mu_B g_{n,JF} m_F |\mathbf{B}_{\text{eff}}|. \quad (12)$$

IV. RESULTS

We consider a ^{87}Rb atom in the $5S_{1/2}, F = 2, m_F = 2$ ground state, which, for the guided mode free-space wavelength $\lambda_{\text{to}} = 790.2$ nm, has a vector polarisability $\alpha_{n,J}^{\text{v}} = 55 \times 10^{-5}$ Hz \cdot m²/V² and a scalar polarisability $\alpha_{n,JF}^{\text{sc}} = 0$ Hz \cdot m²/V², calculated using the Alkali-Rydberg-Calculator (ARC) [54]. We then find $\alpha_{n,JF}^{\text{v}}$ via $\alpha_{n,J}^{\text{v}}$ through the following equation [40]

$$\alpha_{n,JF}^{\text{v}} = (-1)^{J+I+F+1} \sqrt{\frac{2F(2F+1)(J+1)(2J+1)}{2J(F+1)}} \times \begin{Bmatrix} F & 1 & F \\ J & I & J \end{Bmatrix} \alpha_{n,J}^{\text{v}} \quad (13)$$

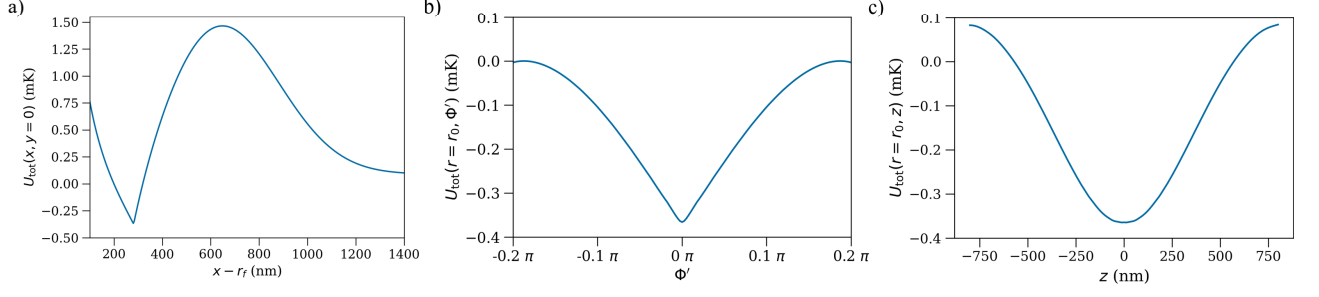


FIG. 4. One-dimensional plots of the light-induced magnetic field trapping potential in (a) radial, $U_{\text{tot}}(x, y = 0)$, (b) azimuthal $U_{\text{tot}}(r = r_0(\Phi'), \Phi')$, and (c) longitudinal, $U_{\text{tot}}(r = r_0(z), z)$, directions for a ^{87}Rb atom in the $|5S_{1/2}, F = 2, m_F = 2\rangle$ ground state. Here, $r_0(\Phi')$ and $r_0(z)$ are the distances from the fibre surface to the trap minimum for fixed values of Φ' and z respectively, see Fig. 3(a,b). Φ' is the adjusted azimuthal component along the trapping potential in the xy plane at the minimum of the trap. The potential is formed by a quasi-linearly polarised fibre guided mode with $P_{\text{ONF}} = 1$ mW and a Gaussian mode tweezers beam with $P_{\text{tw}} = 0.3$ mW. The free-space wavelengths are $\lambda_{\text{ONF}} = 787.3$ nm and $\lambda_{\text{tw}} = 790.2$ nm for the fibre guided mode and tweezers mode, respectively. The fibre radius is $r_f = 175$ nm. Each plot has an offset so that the lowest point represents the trap depth. The trap depth is defined as the minimum potential barrier of the three-dimensional potential $U_{\text{tot}}(x, y, z)$.

to be $\sim 42 \times 10^{-5} \text{ Hz} \cdot \text{m}^2/\text{V}^2$.

The intensity of the tweezers light-induced magnetic field decays along the z -axis from the trapped atom position, see Fig. 2(b,c), while the ONF guided mode field is homogeneous in intensity along the z -axis. Hence, there is no trapping potential created along the z -axis. To overcome this issue, we introduce a detuning to the ONF guided mode wavelength, so that a repulsive force for the ground state atoms is generated. We set λ_{ONF} to 787.3 nm, hence the scalar polarisability, $\alpha_{n,JF}^{\text{sc}} = 15.1 \times 10^{-5} \text{ Hz} \cdot \text{m}^2/\text{V}^2$. The non-zero scalar polarisability results in an attractive potential, U_{sc} . We also include atom-surface interactions using a van der Waals potential, which is non-negligible at distances less than ~ 100 nm from the ONF surface [55]. This is introduced by $U_{\text{vdW}} = -C_3/(r - r_f)^3$, where $C_3 = 3.362 \times 10^{-23} \text{ mK} \cdot \text{m}^3$ for Rb [4] and $r_f = 175$ nm is the ONF radius. Hence, the total potential the atom experiences can be written as

$$\begin{aligned}
 U_{\text{tot}} &= U_{\text{mag}} + U_{\text{sc}} + U_{\text{vdW}} \\
 &= \mu_B g_{n,JF} m_F |\mathbf{B}_{\text{eff}}| - \frac{1}{4} \alpha_{n,JF}^{\text{sc}} |\mathcal{E}_{\text{ONF}}|^2 - \frac{C_3}{(r - r_f)^3}
 \end{aligned} \tag{14}$$

where $|\mathcal{E}_{\text{ONF}}|^2$ is the square of the absolute value of the ONF guided mode electric field amplitude.

We set the polarisation of the ONF guided mode to quasi-linear to increase the intensity of the evanescent field, which increases the amplitude of the light-induced magnetic field at the overlap with the tweezers beam. In addition, using a quasi-linear polarisation creates confinement in the azimuthal direction unlike the quasi-circularly polarised case. The quasi-circular field is homogeneous along the azimuthal direction and therefore does not create a trapping potential along ϕ .

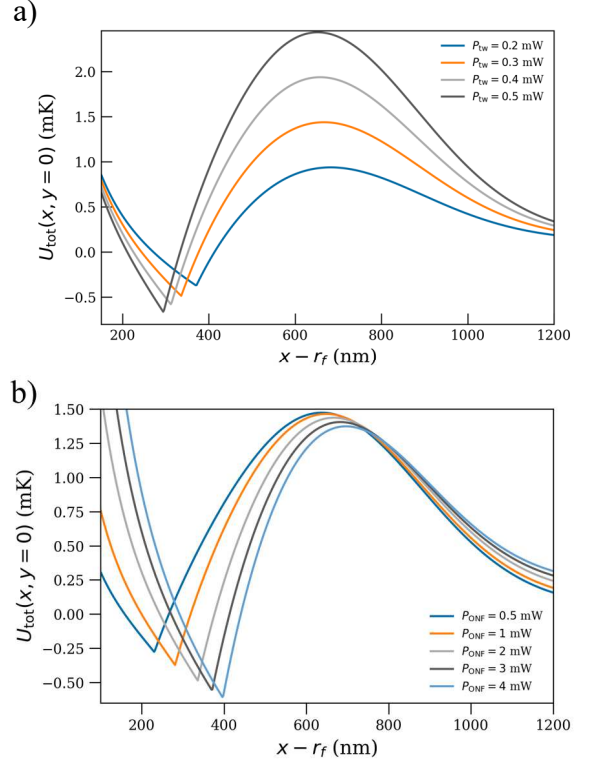


FIG. 5. Radial trapping potentials for the $|5S_{1/2}, F = 2, m_F = 2\rangle$ ground state for (a) $P_{\text{ONF}} = 2.0$ mW and P_{tw} set to 0.2, 0.3, 0.4 and 0.5 mW; (b) $P_{\text{tw}} = 0.3$ mW and P_{ONF} set to 0.5, 1.0, 2.0, 3.0, 4.0 mW. The free-space wavelengths are $\lambda_{\text{ONF}} = 787.3$ nm and $\lambda_{\text{tw}} = 790.2$ nm, respectively. The fibre radius is $r_f = 175$ nm. Each plot has an offset so that the lowest point represents the trap depth. The trap depth is defined as the minimum potential barrier of the three-dimensional potential $U_{\text{tot}}(x, y, z)$.

TABLE I. Parameters for the trapping configurations shown in Fig. 5. P_{ONF} is the ONF guided mode power, P_{tw} is the tweezers power, r_0 is the trap distance from the ONF surface, U_0 is the trap depth, ω_r , $\omega_{\Phi'}$ and ω_z are the radial, azimuthal and longitudinal trapping frequencies, respectively, τ_{trap} is the atom lifetime in the trap. All values are as used in Fig. 5.

P_{ONF} (mW)	P_{tw} (mW)	r_0 (nm)	U_0 (mK)	$\frac{\omega_r}{2\pi}$ (MHz)	$\frac{\omega_{\Phi'}}{2\pi}$ (kHz)	$\frac{\omega_z}{2\pi}$ (kHz)	τ_{trap} (ms)
Gaussian mode optical tweezers							
2	0.2	370	0.37	1.52	57	107	61
2	0.3	336	0.49	2.21	69	121	64
2	0.4	312	0.58	2.27	80	132	64
2	0.5	294	0.66	2.43	90	142	64
1	0.3	281	0.37	2.01	68	114	66
2	0.3	336	0.49	2.21	69	121	64
3	0.3	370	0.55	2.17	70	130	61
4	0.3	396	0.61	2.30	70	140	60

A. Gaussian tweezers

We calculate the total trapping potential for the $|5S_{1/2}, F=2, m_F=2\rangle$ state with the power of the Gaussian tweezers set to 0.3 mW and power of the ONF QL mode set to 1 mW. The centre of the tweezers beam is placed at a distance of 625 nm from the ONF surface, $(x_c, y_c, z_c) = (625, 0, 0)$, with a waist, $w_0 = 0.5 \mu\text{m}$. The QL polarisation of the ONF guided mode is set along the x -axis. The 2D plots of the trapping potential in the xy and xz planes are shown in Fig. 3(a,b), respectively. The minimum of the trapping potential is produced approximately 290 nm away from the surface of the ONF with the depth of the potential $U_{\text{tot}} \approx 0.4$ mK as shown in Fig. 4(a). We also show that the produced potential traps atoms in both the azimuthal (Φ') and longitudinal (z) directions on 1-dimensional plots, see Fig. 4(b,c), respectively.

The trap depth and minimum position strongly depend on both the power of the tweezers beam and the power of the ONF guided light. To illustrate this, we vary the power of the tweezers beam, P_{tw} , from 0.2 mW to 0.5 mW in steps of 0.1 mW while keeping the power of the ONF guided mode, P_{ONF} , constant at 2 mW, see Fig. 5(a). It can be seen that, by changing the power in the tweezers beam, one can easily move the trap minimum from around 370 nm to 290 nm, while increasing the trap depth from 0.3 mK to 0.6 mK. To produce a trapping potential with a similar trap depth using a two-colour fibre-based dipole trap [2] one would need three times more power in the ONF guided mode.

Similarly, we calculate the trapping potentials when keeping the power in the tweezers beam, P_{tw} constant at 0.3 mW and varying the power in the ONF guided mode, P_{ONF} , from 0.5 mW to 4 mW, see Fig. 5(b). The sharp potential arises from the light-induced magnetic field produced by the ONF being cancelled almost to zero by the light-induced magnetic field produced by the tweezers beam. This arises due to the ONF QL mode light-induced magnetic field only being

generated in the xy plane. If the total magnetic field reaches almost zero at the trap minimum, high rates of spin flipping, i.e. changes of the m_F state from positive to negative, can occur. This would be detrimental to the trap lifetime - once the atom changes the sign of the m_F state it is repelled from the trap. For example, for $P_{\text{ONF}} = 2$ mW and $P_{\text{tw}} = 0.4$ mW the spin flip rate, $\Gamma_{\text{sf}} = \frac{\pi\omega_r}{2} \exp\left(-\frac{\pi\mu_B g_{nJ} |\mathbf{B}|}{2\hbar\omega_r}\right)$ [56], is on the order of 10^8 s^{-1} . However, the addition of a quantization magnetic field, which we set to an amplitude of 5 G along the z -axis prevents the loss of atoms from the trap and keeps the spin flip rate on the order of 10^{-4} s^{-1} .

For each configuration we compute the trap depth, U_0 , and trap minimum position relative to the ONF surface, r_0 , the radial, azimuthal and longitudinal trap frequencies, ω_r , $\omega_{\Phi'}$ and ω_z respectively, and the atom lifetime in the trap, $\tau_{\text{trap}} = U_{\text{depth}}/(2E_{\text{rec}}R_{\text{sc}})$ [6], see Table I. R_{sc} is the off-resonant scattering rate from both the tweezers and the ONF electric fields [57].

B. Laguerre-Gaussian tweezers

In the same manner, we calculate the total trapping potential for the $|5S_{1/2}, F=2, m_F=2\rangle$ state with the power of the circularly polarised LG₀₁ ($l=1, p=0$) tweezers beam, P_{LG} , set to 1 mW and the power of the ONF QL mode set to 1 mW. The centre of the tweezers beam is positioned 625 nm away from the ONF surface, with a beam waist of $0.5 \mu\text{m}$. The QL polarisation of the ONF-guided mode is aligned along the x -axis. Figure 6(a,b) shows 2D plots of the trapping potential in the xy and xz planes, respectively. From the radial 1-dimensional plot shown in Fig. 7(a), one can see that the trapping potential reaches a minimum approximately 160 nm from the ONF surface, with a depth of around 1 mK. The 1D trapping potential along the azimuthal (Φ') and longitudinal (z) directions are also shown in Fig. 7(b,c), respectively.

In addition, we look at how the trap depth and the trap minimum position change depending on the power of the LG₀₁ mode tweezers beam while keeping the power of the ONF guided mode, P_{ONF} , constant at 1 mW. To illustrate this, we plot the trapping potential in the radial direction for the power of the tweezers beam, P_{LG} , set to 0.2 mW, 0.3 mW, 0.4 mW and 0.5 mW, see Fig. 8. The trap depth increases from ~ 0.45 mK to ~ 0.96 mK and the trap minimum moves from ~ 250 nm to ~ 160 nm when P_{LG} is changed from 0.2 mW to 0.5 mW. By further increasing the power of the tweezers, one can move the trap minimum to less than 100 nm from the ONF surface, where the van der Waals potential becomes a limiting factor both for the trap depth and the minimum position, see Fig. 7(a).

Similarly, for each power of the LG₀₁ tweezers we compute the trap depth, U_0 , and trap minimum position, r_0 , the radial, azimuthal and longitudinal trap frequencies,

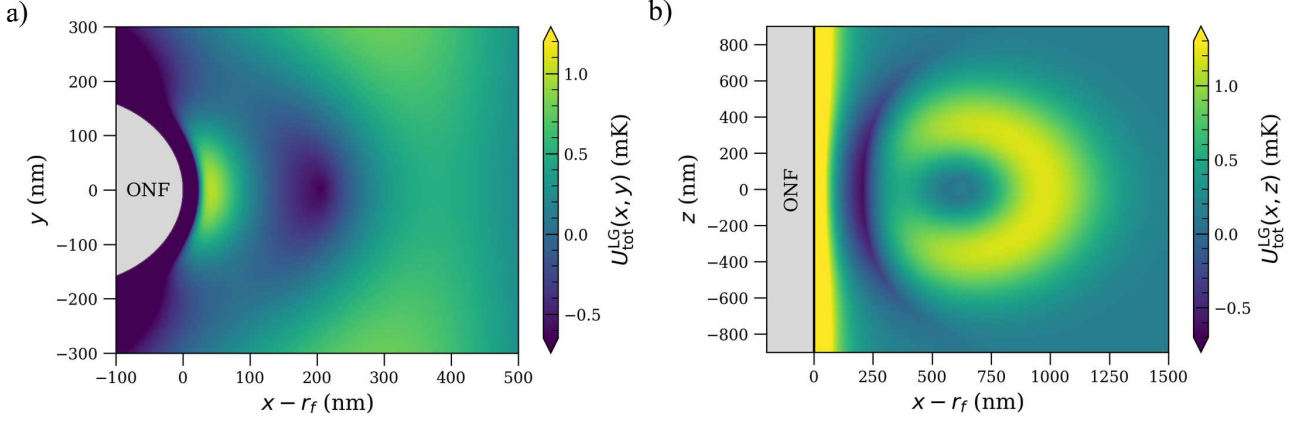


FIG. 6. Two-dimensional plots of the light-induced magnetic field trapping potential (a) $U_{\text{tot}}(x, y)$ and (b) $U_{\text{tot}}(x, z)$, for an atom in the $|5S_{1/2}, F = 2, m_F = 2\rangle$ ground state. The potential is formed by a quasi-linearly polarised fibre guided mode with $P_{\text{ONF}} = 1$ mW and circular polarised LG₀₁ mode tweezers beam with $P_{\text{LG}} = 0.3$ mW. The potential minimum is formed at ~ 208 nm from the fibre surface and the trap depth is ~ 0.65 mK. The free-space wavelengths are $\lambda_{\text{ONF}} = 787.3$ nm and $\lambda_{\text{tw}} = 790.2$ nm for the fibre guided mode and tweezers mode respectively. The fibre radius is $r_f = 175$ nm. Each plot has an offset so that the lowest point represents the trap depth. The trap depth is defined as the minimum potential barrier of the three-dimensional potential $U_{\text{tot}}(x, y, z)$.

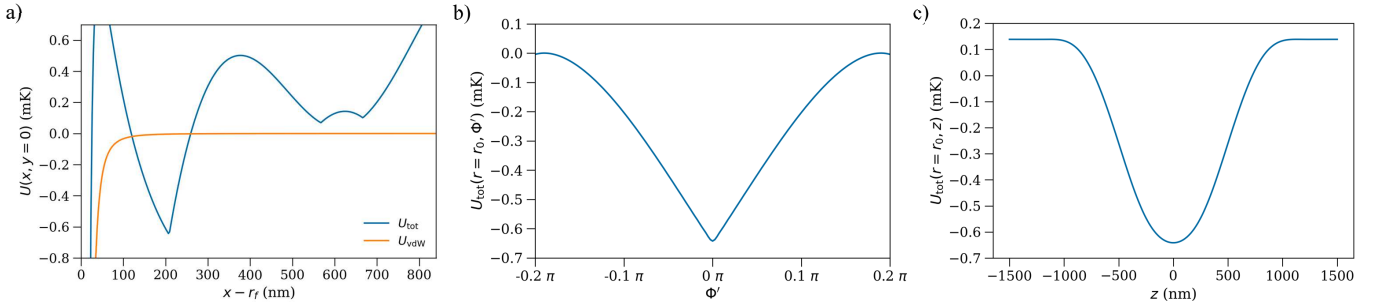


FIG. 7. (a) One-dimensional plots of the van der Waals potential (orange), U_{vdW} , and the light-induced magnetic field trapping potential (blue), $U_{\text{tot}}(x, y = 0)$, in the radial direction. One-dimensional plots of the light-induced magnetic field trapping potential in (b) the azimuthal $U_{\text{tot}}(r = r_0, \Phi')$, and (c) the longitudinal, $U_{\text{tot}}(r = r_0, z)$, directions for an atom in the $|5S_{1/2}, F = 2, m_F = 2\rangle$ ground state. Here Φ' is the adjusted azimuthal component along the trapping potential in the xy plane at the minimum of the trap, $r = r_0$. The potential is formed by a quasi-linearly polarised fibre guided mode with $P_{\text{ONF}} = 1$ mW and LG₀₁ mode tweezers beam with $P_{\text{LG}} = 0.3$ mW. The free-space wavelengths are $\lambda_{\text{ONF}} = 787.3$ nm and $\lambda_{\text{tw}} = 790.2$ nm for the fibre guided mode and tweezers mode respectively. The fibre radius is $r_f = 175$ nm. Each plot has an offset so that the lowest point represents the trap depth. The trap depth is defined as the minimum potential barrier of the three-dimensional potential $U_{\text{tot}}(x, y, z)$.

ω_r , $\omega_{\Phi'}$ and ω_z respectively, and the atom lifetime in the trap $\tau_{\text{trap}} = U_{\text{depth}} / (2E_{\text{rec}}\Gamma_{\text{sc}})$ [6], where Γ_{sc} is the off-resonant scattering rate from both the tweezers and ONF light fields [57], and display them in Table II. It can be observed that increasing the tweezers power results in a deeper trap while the trap lifetime is barely changed, similar to the behaviour seen with Gaussian tweezers, see Table. I. Even with half the power in the ONF mode, the LG tweezers generate a deeper potential than the Gaussian tweezers for the same power, $P_{\text{LG}} = P_{\text{tw}}$. This difference arises from the distinct electric field intensity distributions of the Gaussian and LG₀₁ mode tweezers beams.

TABLE II. Parameters for the trapping configurations shown in Fig. 8. P_{ONF} is the laser power, P_{LG} is the LG₀₁ mode tweezers power, r_0 is the trap distance from the ONF surface, U_0 is the trap depth, ω_r , $\omega_{\Phi'}$ and ω_z are the radial, azimuthal and longitudinal trapping frequencies, respectively, τ_{trap} is the atom lifetime in the trap. All values are as used in Fig. 8.

P_{ONF} (mW)	P_{LG} (mW)	r_0 (nm)	U_0 (mK)	$\frac{\omega_r}{2\pi}$ (MHz)	$\frac{\omega_{\Phi'}}{2\pi}$ (kHz)	$\frac{\omega_z}{2\pi}$ (kHz)	τ_{trap} ms
Laguerre-Gaussian mode optical tweezers							
1	0.2	251	0.45	2.20	44	43	64
1	0.3	208	0.65	2.81	57	82	66
1	0.4	180	0.81	3.26	69	104	67
1	0.5	161	0.96	3.61	79	121	68

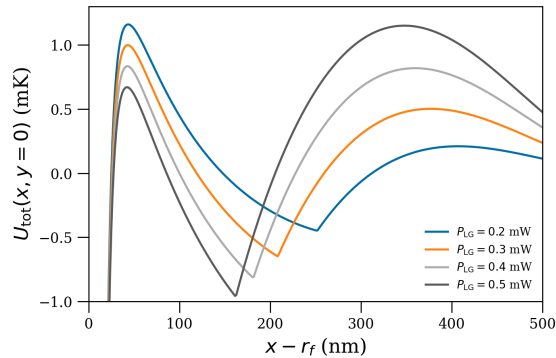


FIG. 8. Radial trap potential for the $|5S_{1/2}, F = 2, m_F = 2\rangle$ ground state for 1 mW power in the fibre guided mode and 0.2, 0.3, 0.4, and 0.5 mW power in the LG_{01} mode tweezers beam. The free-space wavelengths are $\lambda_{\text{ONF}} = 787.3$ nm and $\lambda_{\text{tw}} = 790.2$ nm for the fibre guided mode and tweezers mode, respectively. The fibre radius is $r_f = 175$ nm. Each plot has an offset so that the lowest point represents the trap depth. The trap depth is defined as the minimum potential barrier of the three-dimensional potential $U_{\text{tot}}(x, y, z)$.

In addition, we compare the performance of the two trap configurations created by the Gaussian tweezers beam and the LG_{01} tweezers beam with the same powers, $P_{\text{tw}} = P_{\text{LG}}$, while changing the power of the ONF guided mode, see Fig. 9(a). The LG_{01} tweezers configuration allows for greater adjustment of the trap minimum position than the Gaussian mode tweezers configuration when P_{ONF} is varied. In both cases, the trap depth changes by about 20%, from 0.82 mK to 0.95 mK and from 0.49 mK to 0.42 mK for the LG mode and the Gaussian mode tweezers, respectively. We also compare the two trap configurations with a fixed power of $P_{\text{ONF}} = 1$ mW in the ONF-guided mode, while varying the power in the Gaussian and LG_{01} mode tweezers, as shown in Fig. 9(b). Under these conditions, the LG_{01} mode tweezers configuration provides greater control over both the trap depth and the position of the trap minimum compared to the Gaussian mode configuration.

V. CONCLUSION

In this work, we have studied a novel trapping scheme based on a nanofibre-optical tweezers configuration and provided a detailed analysis of key trap parameters for ^{87}Rb atoms. This scheme is also feasible for other alkali atoms and, in general, for atoms with non-zero vector polarisability and an accessible tune-out wavelength for the scalar light shift. The proposed magnetic trap achieves depths sufficient for trapping laser-cooled atoms, using optical powers comparable to those required for conventional two-colour nanofibre traps and optical tweezers. Our scheme provides several key advantages over the configuration where an optical tweezers illuminates an opti-

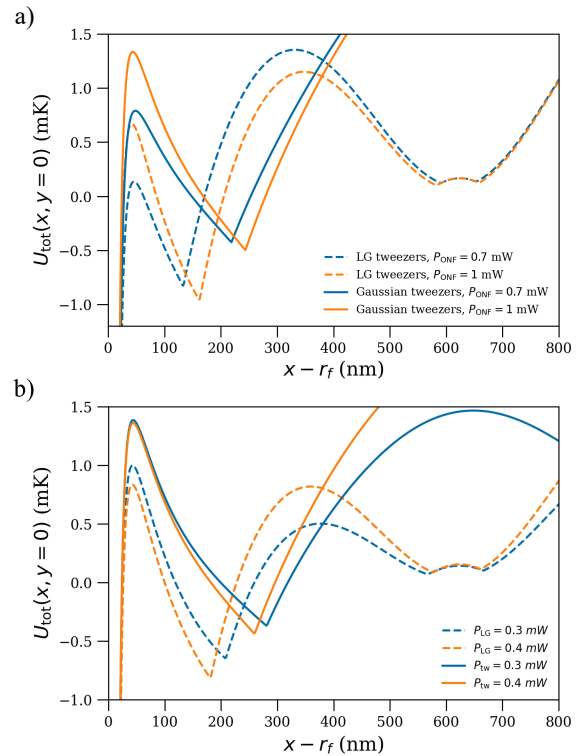


FIG. 9. Radial trap potential for the $5|S_{1/2}, F = 2, m_F = 2\rangle$ ground state for a) 0.5 mW of power in the LG_{01} (dashed lines) and Gaussian mode (solid lines) tweezers beams and 0.7 mW (blue) and 1 mW (orange) of power in the ONF guided mode; b) 1 mW of power in the ONF guided mode, 0.3 mW (blue) and 0.4 mW (orange) power in the LG_{01} (dashed lines) and Gaussian mode (solid lines) tweezers beams. The free-space wavelengths are $\lambda_{\text{ONF}} = 787.3$ nm and $\lambda_{\text{tw}} = 790.2$ nm for the fibre guided mode and tweezers modes, respectively. The fibre radius is $r_f = 175$ nm. Each plot has an offset so that the lowest point represents the trap depth. The trap depth is defined as the minimum potential barrier of the three-dimensional potential $U_{\text{tot}}(x, y, z)$.

cal waveguide, creating a standing-wave dipole potential for trapping an atom. Our scheme allows for significant tunability of the trap minimum position relative to the waveguide surface, enabling adjustable coupling of light emitted by the trapped atoms into the fibre-guided mode. Additionally, it avoids the need for direct illumination of the ONF by the tweezers light, thereby diminishing the risk of ONF damage from heat dissipation caused by scattered light. In our scheme, the atom position—or trap minimum—can be readily adjusted as the powers of both the ONF-guided mode and the optical tweezers are controlled via an acousto-optic modulator. When manipulating trapped atoms one should change the trap position in an adiabatic manner compared to the trap frequencies. The calculated trap frequencies and AOM rise times allow for the proposed scheme to make adjustments on timescales comparable to AOD-based optical tweezers.

We analysed and compared the trap configurations for both Gaussian and Laguerre-Gaussian mode tweezers beams. We concluded that the Laguerre-Gaussian tweezers provides greater control over the trap depth, as well as the minimum trap position from the ONF surface in comparison to the Gaussian mode tweezers. Additionally, we demonstrated that the LG mode tweezers offers a deeper trap compared to the Gaussian mode at similar powers. This advantage arises from the different intensity distributions between the LG and Gaussian modes.

In typical configurations of our proposed ONF-tweezers light-induced magnetic field trap, the trap minimum is positioned 100–400 nm from the ONF surface, with trap depths ranging from 0.3 to 1 mK. The trap depth of more than 0.3 mK enables the loading of atoms that have been laser-cooled using a magneto-optical trap. Since we do not exploit external magnetic fields to create minima of the light-induced magnetic field but solely optical fields, we can load atoms directly from

a MOT, which is an advantage over the technique proposed in [41], where atoms have to be loaded from a conventional two-colour dipole trap.

ACKNOWLEDGMENTS

The authors would like to thank the Scientific Computing and Data Analysis Section at OIST. This work was supported by funding from the Okinawa Institute of Science and Technology Graduate University. S.N.C. acknowledges support from the Japan Society for the Promotion of Science (JSPS) Grant-in-Aid No. 24K08289, respectively.

DATA AVAILABILITY STATEMENT

The data is available from the corresponding authors upon reasonable request.

-
- [1] V. Balykin, K. Hakuta, F. Le Kien, J. Liang, and M. Morinaga, Atom trapping and guiding with a subwavelength-diameter optical fiber, *Phys. Rev. A* **70**, 011401 (2004).
- [2] E. Vetsch, D. Reitz, G. Sagué, R. Schmidt, S. Dawkins, and A. Rauschenbeutel, Optical interface created by laser-cooled atoms trapped in the evanescent field surrounding an optical nanofiber, *Phys. Rev. Lett.* **104**, 203603 (2010).
- [3] J. D. Thompson, T. Tiecke, N. P. de Leon, J. Feist, A. Akimov, M. Gullans, A. S. Zibrov, V. Vuletić, and M. D. Lukin, Coupling a single trapped atom to a nanoscale optical cavity, *Science* **340**, 1202 (2013).
- [4] M. Daly, V. G. Truong, C. Phelan, K. Deasy, and S. Nic Chormaic, Nanostructured optical nanofibres for atom trapping, *New J. Phys.* **16**, 053052 (2014).
- [5] E. Da Ros, N. Cooper, J. Nute, and L. Hackermueller, Cold atoms in micromachined waveguides: A new platform for atom-photon interactions, *Phys. Rev. Res.* **2**, 033098 (2020).
- [6] F. Le Kien, S. Nic Chormaic, and T. Busch, Optical trap for an atom around the midpoint between two coupled identical parallel optical nanofibers, *Phys. Rev. A* **103**, 063106 (2021).
- [7] A. Bouscal, M. Kemiche, S. Mahapatra, N. Fayard, J. Berroir, T. Ray, J.-J. Greffet, F. Raineri, A. Levenson, K. Bencheikh, *et al.*, Systematic design of a robust half-w1 photonic crystal waveguide for interfacing slow light and trapped cold atoms, *New J. Phys.* **26**, 023026 (2024).
- [8] W. Li, D. Brown, A. Vylegzhanin, Z. Shahrabifarahani, A. Raj, J. Du, and S. Nic Chormaic, Atom-light interactions using optical nanofibres—a perspective, *JPhys: Photonics* **6**, 021002 (2024).
- [9] A. Goban, K. Choi, D. Alton, D. Ding, C. Lacroûte, M. Pototschnig, T. Thiele, N. Stern, and H. Kimble, Demonstration of a state-insensitive, compensated nanofiber trap, *Phys. Rev. Lett.* **109**, 033603 (2012).
- [10] D. H. White, S. Kato, N. Német, S. Parkins, and T. Aoki, Cavity dark mode of distant coupled atom-cavity systems, *Phys. Rev. Lett.* **122**, 253603 (2019).
- [11] J. Lee, J. A. Grover, J. E. Hoffman, L. A. Orozco, and S. L. Rolston, Inhomogeneous broadening of optical transitions of ^{87}Rb atoms in an optical nanofiber trap, *J. Phys. B: At. Mol. Opt. Phys.* **48**, 165004 (2015).
- [12] R. K. Gupta, J. L. Everett, A. D. Tranter, R. Henke, V. Gokhroo, P. K. Lam, and S. Nic Chormaic, Machine learner optimization of optical nanofiber-based dipole traps, *AQS* **4**, 026801 (2022).
- [13] G. Sagué, E. Vetsch, W. Alt, D. Meschede, and A. Rauschenbeutel, Cold-atom physics using ultrathin optical fibers: Light-induced dipole forces and surface interactions, *Phys. Rev. Lett.* **99**, 163602 (2007).
- [14] L. Russell, K. Deasy, M. J. Daly, M. J. Morrissey, and S. Nic Chormaic, Sub-Doppler temperature measurements of laser-cooled atoms using optical nanofibres, *Meas. Sci. Technol.* **23**, 015201 (2011).
- [15] J. Lee, D. Park, S. Mittal, M. Dagenais, and S. Rolston, Integrated optical dipole trap for cold neutral atoms with an optical waveguide coupler, *New J. Phys.* **15**, 043010 (2013).
- [16] R. Kumar, V. Gokhroo, K. Deasy, and S. Nic Chormaic, Autler-Townes splitting via frequency up-conversion at ultralow-power levels in cold ^{87}Rb atoms using an optical nanofiber, *Phys. Rev. A* **91**, 053842 (2015).
- [17] S. Kato, N. Német, K. Senga, S. Mizukami, X. Huang, S. Parkins, and T. Aoki, Observation of dressed states of distant atoms with delocalized photons in coupled-cavities quantum electrodynamics, *Nat. Commun.* **10**, 1160 (2019).
- [18] T. Ray, R. K. Gupta, V. Gokhroo, J. L. Everett, T. Nieddu, K. S. Rajasree, and S. Nic Chormaic, Observation of the ^{87}Rb $5S_{1/2}$ to $4D_{3/2}$ electric quadrupole transition at 516.6 nm mediated via an optical nanofibre,

- New J. Phys. **22**, 062001 (2020).
- [19] E. Stourm, M. Lepers, J. Robert, S. Nic Chormaic, K. Mølmer, and E. Brion, Spontaneous emission and energy shifts of a Rydberg rubidium atom close to an optical nanofiber, *Phys. Rev. A* **101**, 052508 (2020).
- [20] K. S. Rajasree, T. Ray, K. Karlsson, J. L. Everett, and S. Nic Chormaic, Generation of cold Rydberg atoms at submicron distances from an optical nanofiber, *Phys. Rev. Res.* **2**, 012038 (2020).
- [21] E. Stourm, M. Lepers, J. Robert, S. Nic Chormaic, K. Moelmer, and E. Brion, Interaction of two Rydberg atoms in the vicinity of an optical nanofibre, *New J. Phys.* **25**, 023022 (2023).
- [22] A. Vylegzhanin, D. J. Brown, A. Raj, D. F. Koroňanov, J. L. Everett, E. Brion, J. Robert, and S. Nic Chormaic, Excitation of ^{87}Rb Rydberg atoms to $n\text{S}$ and $n\text{D}$ states ($n \leq 68$) via an optical nanofiber, *Optica Quantum* **1**, 6 (2023).
- [23] L. Zhang, F. Yang, K. Mølmer, and T. Pohl, Chiral quantum-optical elements for waveguide-QED with sub-wavelength Rydberg-atom arrays, arXiv preprint arXiv:2407.01133 (2024).
- [24] T. Wilk, A. Gaëtan, C. Evellin, J. Wolters, Y. Miroshnychenko, P. Grangier, and A. Browaeys, Entanglement of two individual neutral atoms using Rydberg blockade, *Phys. Rev. Lett.* **104**, 010502 (2010).
- [25] M. Ebert, M. Kwon, T. Walker, and M. Saffman, Coherence and Rydberg blockade of atomic ensemble qubits, *Phys. Rev. Lett.* **115**, 093601 (2015).
- [26] G. Calajó, F. Ciccarello, D. Chang, and P. Rabl, Atom-field dressed states in slow-light waveguide QED, *Phys. Rev. A* **93**, 033833 (2016).
- [27] I. Cong, H. Levine, A. Keesling, D. Bluvstein, S.-T. Wang, and M. D. Lukin, Hardware-efficient, fault-tolerant quantum computation with Rydberg atoms, *Phys. Rev. X* **12**, 021049 (2022).
- [28] L. Heller, J. Lowinski, K. Theophilo, A. Padrón-Brito, and H. de Riedmatten, Raman storage of quasideterministic single photons generated by Rydberg collective excitations in a low-noise quantum memory, *Phys. Rev. Applied* **18**, 024036 (2022).
- [29] D. Frese, B. Ueberholz, S. Kuhr, W. Alt, D. Schrader, V. Gomer, and D. Meschede, Single atoms in an optical dipole trap: Towards a deterministic source of cold atoms, *Phys. Rev. Lett.* **85**, 3777 (2000).
- [30] J. Beugnon, C. Tuchendler, H. Marion, A. Gaëtan, Y. Miroshnychenko, Y. R. Sortais, A. M. Lance, M. P. Jones, G. Messin, A. Browaeys, *et al.*, Two-dimensional transport and transfer of a single atomic qubit in optical tweezers, *Nat. Phys.* **3**, 696 (2007).
- [31] A. M. Kaufman, B. J. Lester, and C. A. Regal, Cooling a single atom in an optical tweezer to its quantum ground state, *Phys. Rev. X* **2**, 041014 (2012).
- [32] K.-N. Schymik, V. Lienhard, D. Barredo, P. Scholl, H. Williams, A. Browaeys, and T. Lahaye, Enhanced atom-by-atom assembly of arbitrary tweezer arrays, *Phys. Rev. A* **102**, 063107 (2020).
- [33] H. J. Manetsch, G. Nomura, E. Bataille, K. H. Leung, X. Lv, and M. Endres, A tweezer array with 6100 highly coherent atomic qubits, arXiv preprint arXiv:2403.12021 (2024).
- [34] D. Barredo, V. Lienhard, P. Scholl, S. de Léséleuc, T. Boulier, A. Browaeys, and T. Lahaye, Three-dimensional trapping of individual Rydberg atoms in ponderomotive bottle beam traps, *Phys. Rev. Lett.* **124**, 023201 (2020).
- [35] J. Wilson, S. Saskin, Y. Meng, S. Ma, R. Dilip, A. Burgers, and J. Thompson, Trapping alkaline earth Rydberg atoms optical tweezer arrays, *Phys. Rev. Lett.* **128**, 033201 (2022).
- [36] K. P. Nayak, J. Wang, and J. Keloth, Real-time observation of single atoms trapped and interfaced to a nanofiber cavity, *Phys. Rev. Lett.* **123**, 213602 (2019).
- [37] J.-B. Béguin, J. Laurat, X. Luan, A. Burgers, Z. Qin, and H. J. Kimble, Reduced volume and reflection for bright optical tweezers with radial Laguerre-Gauss beams, *PNAS* **117**, 26109 (2020).
- [38] K. J. Mitchell, S. Turtaev, M. J. Padgett, T. Čížmár, and D. B. Phillips, High-speed spatial control of the intensity, phase and polarisation of vector beams using a digital micro-mirror device, *Opt. Express* **24**, 29269 (2016).
- [39] E. Cohen-Tannoudji and J. Dupont-Roc, Experimental study of Zeeman light shifts in weak magnetic fields, *Phys. Rev. A* **5**, 968 (1972).
- [40] F. Le Kien, P. Schneeweiss, and A. Rauschenbeutel, Dynamical polarizability of atoms in arbitrary light fields: general theory and application to cesium, *EPJD* **67**, 1 (2013).
- [41] P. Schneeweiss, F. Le Kien, and A. Rauschenbeutel, Nanofiber-based atom trap created by combining fictitious and real magnetic fields, *New J. Phys.* **16**, 013014 (2014).
- [42] D. Barredo, S. de Léséleuc, V. Lienhard, T. Lahaye, and A. Browaeys, An atom-by-atom assembler of defect-free arbitrary two-dimensional atomic arrays, *Science* **354**, 1021 (2016).
- [43] F. Le Kien, P. Schneeweiss, and A. Rauschenbeutel, Dynamical polarizability of atoms in arbitrary light fields: general theory and application to cesium, *EPJD* **67**, 92 (2013).
- [44] L. LeBlanc and J. Thywissen, Species-specific optical lattices, *Phys. Rev. A* **75**, 053612 (2007).
- [45] M. C. Frawley, A. Petcu-Colan, V. G. Truong, and S. Nic Chormaic, Higher order mode propagation in an optical nanofiber, *Opt. Commun.* **285**, 4648 (2012).
- [46] F. Le Kien, T. Busch, V. G. Truong, and S. Nic Chormaic, Higher-order modes of vacuum-clad ultrathin optical fibers, *Phys. Rev. A* **96**, 023835 (2017).
- [47] F. Le Kien, J. Liang, K. Hakuta, and V. Balykin, Field intensity distributions and polarization orientations in a vacuum-clad subwavelength-diameter optical fiber, *Opt. Commun.* **242**, 445 (2004).
- [48] F. Le Kien, P. Schneeweiss, and A. Rauschenbeutel, State-dependent potentials in a nanofiber-based two-color trap for cold atoms, *Phys. Rev. A* **88**, 033840 (2013).
- [49] S. Zhang, F. Robicheaux, and M. Saffman, Magic-wavelength optical traps for Rydberg atoms, *Phys. Rev. A* **84**, 043408 (2011).
- [50] K. Corwin, S. Kuppens, D. Cho, and C. Wieman, Spin-polarized atoms in a circularly polarized optical dipole trap, *Phys. Rev. Lett.* **83**, 1311 (1999).
- [51] G. Yang, H. Yan, T. Shi, J. Wang, M. Zhan, *et al.*, Optically induced fictitious magnetic trap on an atom chip, *Phys. Rev. A* **78**, 033415 (2008).
- [52] M. Zielonkowski, J. Steiger, U. Schünemann, M. DeKieviet, and R. Grimm, Optically induced spin precession and echo in an atomic beam, *Phys. Rev.*

- A **58**, 3993 (1998).
- [53] C. Y. Park, J. Y. Kim, J. M. Song, and D. Cho, Optical Stern-Gerlach effect from the Zeeman-like ac Stark shift, *Phys. Rev. A* **65**, 033410 (2002).
- [54] E. J. Robertson, N. Šibalić, R. M. Potvliege, and M. P. Jones, Arc 3.0: An expanded Python toolbox for atomic physics calculations, *Comput. Phys. Commun.* **261**, 107814 (2021).
- [55] V. G. Minogin and S. Nic Chormaic, Manifestation of the van der Waals surface interaction in the spontaneous emission of atoms into an optical nanofiber, *Laser Phys.* **20**, 32 (2010).
- [56] C. Sukumar and D. M. Brink, Spin-flip transitions in a magnetic trap, *Phys. Rev. A* **56**, 2451 (1997).
- [57] J. Bai, S. Liu, J. He, and J. Wang, Towards implementation of a magic optical-dipole trap for confining ground-state and Rydberg-state cesium cold atoms, *J. Phys. B: At. Mol. Opt. Phys.* **53**, 155302 (2020).